Biomaterials and Biomechanics in Bioengineering, *Vol. 1, No. 4 (2014) 175-188*
(Formerly, Advances in Biomechanics and Applications)
DOI: http://dx.doi.org/10.12989/bme.2014.1.4.175

3D finite element simulation of human proximal femoral fracture under quasi-static load

Ridha Hambli*

Prisme Institute - MMH 8, Rue Leonard de Vinci, 45072, Orleans cedex 2, France

(Received June 14, 2012, Revised February 6, 2013, Accepted February 13, 2012)

Abstract. In this paper, a simple and accurate finite element model coupled to quasi-brittle damage law able to describe the multiple cracks initiation and their progressive propagation is developed in order to predict the complete force-displacement curve and the fracture pattern of human proximal femur under quasi-static load. The motivation of this work was to propose a simple and practical FE model with a good compromise between complexity and accuracy of the simulation considering a limited number of model parameters that can predict proximal femur fracture more accurately and physically than the fracture criteria based models. Different damage laws for cortical and trabecular bone are proposed based on experimental results to describe the inelastic damage accumulation under the excessive load. When the damage parameter reaches its critical value inside an element of the mesh, its stiffness matrix is set to zero leading to the redistribution of the stress state in the vicinity of the fractured zone (crack initiation). Once a crack is initiated, the propagation direction is simulated by the propagation of the broken elements of the mesh. To illustrate the potential of the proposed approach, the left femur of a male (age 61) previously investigated by Keyak and Falkinstein, 2003 (Model B: male, age 61) was simulated till complete fracture under one-legged stance quasi-static load. The proposed finite element model leads to more realistic and precise results concerning the shape of the force-displacement curve (yielding and fracturing) and the profile of the fractured edge.

Keywords: finite element; proximal femur fracture; crack propagation; fracture pattern; force-displacement curve

1. Introduction

In order to predict fracture conditions (maximum fracture load and fracture pattern), linear and non-linear finite element (FE) models were developed in mechanical studies of proximal femur (Cody *et al*. 1999, Keyak 2001, Keyak and Falkinstein 2003, Schileo *et al*. 2008, Lotz *et al*. 1991a, 1991b, 1995, Ota *et al*. 1999, Crawford *et al*. 2003, Ford *et al*.1996, Taddei *et al*. 2006, Bessho *et al*. 2007, Schileo *et al*. 2008, Dragomir-Daescu *et al*. 2011, Juszczyk *et al*. 2011). Different fracture criteria were applied in the previous studies in order to predict the onset of the bone fracture under excessive load without coupling the effect of the damage during fracturing process and the mechanical behaviour of bone. Such criteria are suitable in general for ductile material. It is well admitted that the tensile strength of bone is smaller than its compressive strength

*Corresponding author, Professor, E-mail: ridha.hambli@univ-orleans.fr

http://www.techno-press.org/?journal=aba&subpage=7 ISSN: 2287-2094 (Print), 2287-2272 (Online)

suggesting that it exhibits a quasi-brittle material behaviour (Reilly and Burstein 1975, Keaveny *et al.* 1999, Currey 2002, Kaneko *et al.*2003, Kotha and Guzelsu 2003, Bayraktar *et al.* 2004). Experiment of Keaveny *et al.*(1999) showed a typical quasi-brittle stress-strain relation of bone. In addition, such criteria based models allow the simulation proximal femoral fracture from initial loading, to the start of local bone failure without considering the loss of bone material stiffness generated by the progressive damage accumulation prior fracture. However, a shortcoming of these models is that the damage growth and cracks propagation within bone leading to complete fracture are not simulated. Hence, the computed force–displacement curves based on these models did not exhibit the sharp drop in force usually seen during mechanical testing and the femur fracture pattern were not be predicted in realistic ways.

Recently, several authors investigated the fracture of cortical bone based on fracture mechanics concepts (Malik *et al.* 2003, Nalla *et al.* 2005, Vashishth *et al.* 1997, 2003, Yang *et al.* 2006, Ural and Vashishth 2007, Abdel-Wahab and Silberschmidt 2011). The major limitations of application of the fracture mechanics methods to simulate realistically whole bone fracture is related to the fact that the methods are only valid for the of a single dominant crack with a cohesive zone (Yang *et al.* 2006).

Previous fracture criteria based models and fracture mechanics models are not able to simulate the cracks initiation and their progressive propagation leading to the complete fracture of bone organ under excessive load in realistic and simple ways. At yielding and subsequent failure, bone may show post-yielding (quasi-brittle) behaviour (Keaveny *et al.* 2001) or immediate failure (brittle behaviour) (Schileo *et al.* 2008, Juszczyk *et al.* 2011). In spite of the large number of FE studies dealing with bone fracture under monotonic load, there is still a lack of practical and simple FE models considering the complete and realistic behaviour of bone from elastic stage till complete fracture. Such models can be developed incorporating the continuum damage mechanics (CDM) concept in order to predict the progressive cracks initiation and propagation leading to complete fracture of bone organ. Such approaches allow for the prediction of fracture pattern and the whole force-displacement curve (from elastic stage till complete fracture). In addition, fracture represents the terminal manifestation of the loading process. However, damaging of bone during loading process should be considered for realistic and physical simulation of bone behaviour subjected to fracturing. Also, bone, as a biological tissue, possesses a very complex hierarchical structure.

In the present work, an isotropic FE model coupled to quasi-brittle damage law was developed in order to simulate the progressive fracturing process of human proximal femurs under quasi-static load and predict the complete force-displacement curve and the final fracture pattern of the proximal femur under one-legged stance load. Different damage laws for cortical and trabecular bone are proposed based on experimental results to describe the inelastic damage accumulation under the excessive load. When the damage parameter reaches its critical value inside an element of the mesh, its stiffness matrix is set to zero leading to the redistribution of the stress state in the vicinity of the fractured zone (crack initiation). The propagation of a crack is simulated by the propagation of the broken elements of the mesh. The current isotropic strategy is motivated by: (i) Some published comparative studies claiming that the assigned orthotropic material model has a limited effect on the FE result at bone organ level compared to the isotropic one (Peng *et al.* 2006, Verhulp *et al.* 2006, Baca *et al.* 2008), and (ii) the complexity regarding the assignment of the local anisotropic directions for every FE of the mesh and their corresponding anisotropic material properties (Tellache *et al.* 2009, San Antonio *et al.* 2012).

To illustrate the potential of the proposed approach, the left femur of a male (age 61) previously

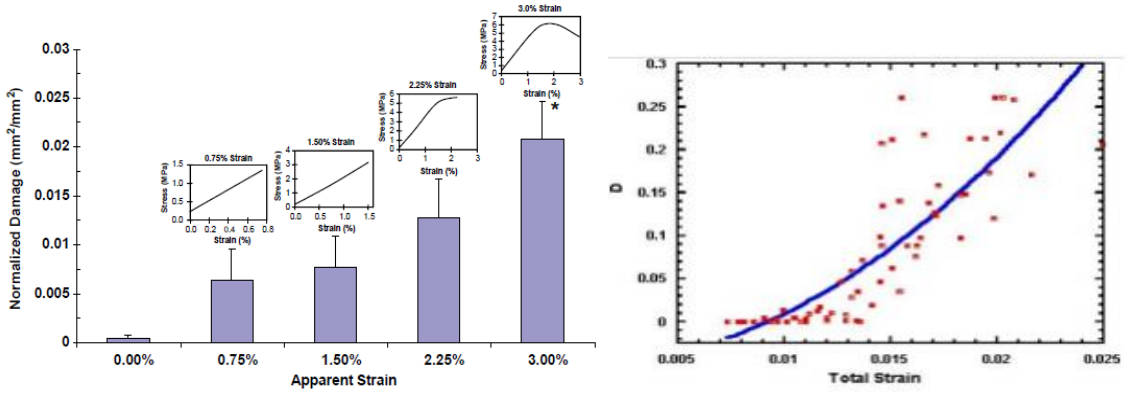

(a) Trabecular bone damage from Nagaraja *et al.*(2005) (b) Cortical bone damage from Parsamian (2002)

Fig. 1 Damage evolution versus apparent strain: (a) Damage of trabecular bone and corresponding stress-strain curve under uniaxial compressive behaviour in overloading situation performed by Nagaraja *et al.*(2005). (b) Damage of cortical bone under uniaxial compressive behaviour performed by Parsamian, (2002)

investigated by Keyak and Falkinstein (2003) (Model B) was simulated till complete fracture under one-legged stance load. The proposed damaged model leads to more precise and realistic results concerning the shape of the force-displacement curve (yielding and fracturing) and the fracture pattern.

2. Method

2.1 Quasi-brittle behaviour law of bone under quasi-static load

Human femurs can experience brittle behaviour (Link *et al.* 2003, Yang *et al.* 1996, Schileo *et al.* 2008, Juszczyk *et al.* 2011) to quasi-brittle failure behaviour (Keyak 2001, Keyak and Falkinstein 2003, Bessho *et al.* 2007, Dragomir-Daescu *et al.* 2011) depending mainly on bone organ geometry and intrinsic properties, viscosity, specimen preparation (fresh frozen, embalmed), aging (decrease of toughness of bone) and the load testing speed. In general, at a low rate load (quasi-static regime), proximal femur organ behave as a quasi-brittle material with a non-linear behaviour till complete fracture (Keyak 2001, Keyak and Falkinstein 2003, Bessho *et al.* 2007, Dragomir-Daescu *et al.* 2011). At high rate load (typically 30 mm/s), proximal femurs have linear-elastic behaviour up to fracture followed by a sharp decrease of load after reaching the maximum value.

Fig. 1 shows an example of the experimental quasi-brittle damage evolution of trabecular and cortical bone under compressive overloading situation obtained respectively by Nagaraja *et al.*(2005) and Parsamian (2002).

In the quasi-static regime without considering the viscosity effects, the stress-strain relation of elasticity based damage mechanics is expressed by (Chaboche 1981, Lemaitre 1985)

$$\sigma_{ij} = (1-D)C_{ijkl}\varepsilon_{kl} \tag{1}$$

Where D denote the damage variable, σ_{ij} the stress components, ε_{kl} the strains and C_{ijkl} are the components of elasticity tensor.

Relation (1) shows that the damage variable acts as a stiffness reduction factor. For increasing damage, the effective stiffness moduli $(1-D)C_{ijkl}$ decrease.

The growth of the quasi-brittle damage variable is controlled by the damage threshold parameter κ, which is defined as the maximum of the equivalent strain measure ε_{eq} reached during the load history

$$\kappa = \max(\varepsilon_{eq}) \tag{2}$$

the equivalent strain ε_{eq} is expressed by

$$\varepsilon_{eq} = \sqrt{\frac{2}{3}\varepsilon_{ij}\varepsilon_{ij}} \tag{3}$$

Damage growth depends on a damage loading function in terms of the strain components expressed by (Mazars *et al.* 1996)

$$f(\varepsilon_{eq}, \varepsilon_0) = \varepsilon_{eq} \quad \max(\kappa, \varepsilon_0) \tag{4}$$

Where ε_0 is the initial value of κ when damage starts. If the loading function *f* is negative, damage does not develop. During monotonic loading, the parameter κ grows (it coincides with ε_{eq}) and during unloading and reloading it remains constant:

$f < 0$: No damage growth and the material behaviour is elastic.

$f \geq 0$: Damage growth and reduction of the stiffness.

When the condition ($f \geq 0$) is satisfied, the growth of damage is governed by an evolution law which expressed in the general form (Lemaitre 1985)

$$\dot{D} = g(D, \varepsilon_{eq}, \sigma_{ij})\dot{\varepsilon}_{eq} \tag{5}$$

2.2 Damage laws of trabecular and cortical bone

Considering the experimental results of Wolfram *et al.*(2011) performed on 251 cylindrical trabecular bone samples obtained from human vertabrae (T1-L3) and the results performed on human cortical bone by Parsamian (2002) (Fig. 2), an experimentally fitted damage law can be expressed in the general

$$\begin{cases} D = 0 & ; \varepsilon_{eq} \leq \varepsilon_0 \\ D = D_c\ \varepsilon_{eq}^n & ; \varepsilon_0 < \varepsilon_{eq} < \varepsilon_f \\ D = D_c & ; \varepsilon_{eq} \geq \varepsilon_f \end{cases} \tag{6}$$

D_c, n and ε_f are respectively the critical damage at fracture, the damage exponent and the strain at fracture which can be assessed based on experimental results (Parsamian 2002, Wolfram

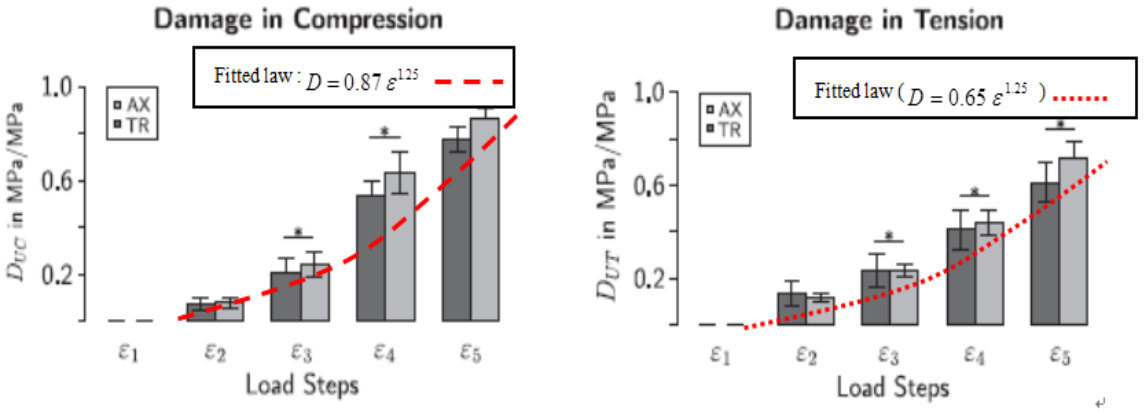

(a) Experimental averaged damage in tension and compression performed on 251 human vertabrae trabecular specimens (Wolfram *et al.*2011) and computed fitted damage laws in compression and tension based on the experimental results

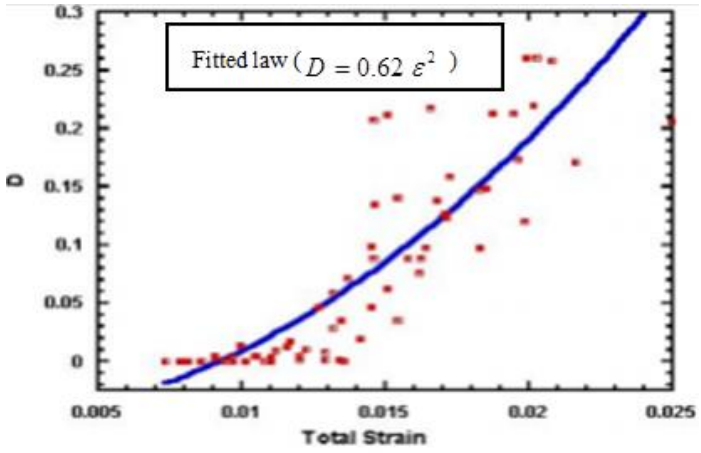

(b) Experimental averaged damage law for human cortical bone performed on fourteen cortical cores specimens (Parsamian, 2002) and corresponding fitted damage law

Fig. 2 Damage laws for human trabecular and cortical bone from reported literature

et al. 2011) (Fig. 2 and Table 1). The constants in Eq. (5) were determined by a trial and error optimization procedure to improve the agreement between fitted and experimental damage laws of Fig. 2(a) and 2(b).

In addition, numerous studies show that damage threshold strains and stresses of trabecular and cortical bone tissue are different in tension and compression (Reilly and Burstein 1974, 1975, Currey 1990, Kotha and Guzelsu 2003, Keaveny *et al.* 1994, 1999, 2001, Wolfram *et al.* 2011). Therefore, to account for the asymmetrical bone yields, the strain at fracture is given by

$$\begin{cases} \varepsilon_f = \varepsilon_f^T \quad and \quad D_c = D_c^T \quad in \ \ Tension \\ \varepsilon_f = \varepsilon_f^C \quad and \quad D_c = D_c^C \quad in \ \ Compressio \ n \end{cases} \tag{7}$$

ε_f^T and ε_f^C are the tensile and compressive strain at fracture respectively.
D_c^T and D_c^C are critical damage values at fracture in tension and compression.

2.3 Crack propagation simulation

A practical and accurate enough way to represent fracture is the so-called '*kill element*' technique (Hambli 2011a, 2011b). With the concept of CDM, there is no difference between crack initiation and propagation. Both of are resulted from the failure of an element of the mesh. Thus, crack initiation and propagation are studied as unified approach (Chaboche 1981, Lemaitre 1985). Similar approach was developed by Wang *et al.* (2008a, 2008b) to simulate microcracks propagation of iliac crest bone specimens using 2D FE model.

The current developed technique distinguishes between tension, shearing and compression loading modes as follow:

In tension:

When the damage parameter reaches its critical value D_c^T inside an element, its stiffness matrix is set to zero leading to the redistribution of the stress state in the vicinity of the fractured zone (crack initiation). Once a crack is initiated the propagation direction is simulated by the propagation of the broken elements of the mesh. At continuum level, the local critical damage value in tension is generally equal to 1 ($D_c^T \approx 1.0$) (Zioupos *et al.* 1996, Pattin *et al.* 1996). To avoid numerical convergence problems, the critical damage value at fracture was set to $D_c^T = 0.95$.

In compression and shearing:

When the kill element method is used in compressive or shearing regions, modeling the self-contact as the gap created the element removal is need. The alternative is to keep the elements, but to lower their stiffness to a low, but not null value. In compression and shearing, the critical damage value at fracture was set to $D_c^C = 0.5$ (Hambli 2011a, 2011b).

3. Fracture simulation of proximal femur under one-legged stance quasi-static load

To illustrate the potential of the proposed FE model to predict the complete force-displacement curve and the fracture pattern, we simulated the ex-vivo experimental test performed previously by Keyak and Falkinstein (2003) (Model B) (Fig. 3(a)). The authors tested among others a left femur of a male (age 61) under one-legged stance load till complete fracture.

In current case, the 3D FE model was generated automatically from the geometry of the femur of a 60 year old male scanned to obtain a set of slices by quantitative computed tomography (QCT) using software developed in-house based on a two-step procedure. First, the contours of the femur are extracted from the CT scan. Based on these contours, the surface of the bone is reconstructed, from which, in a second step, a FE mesh with 33150 parabolic tetrahedral elements is built (Fig. 3(b)). Same loads and boundary conditions were applied to the femur than in the experimental work of Keyak and Falkinstein (2003). Note that the FE model constructed for the simulation is different from Keyak and Falkinstein (2003) one. Each individual femur geometry and mechanical properties are different in term of mechanical response and fracture generated by applied loads due. Nevertheless, same bone properties of same age were assigned and the overall structure of the

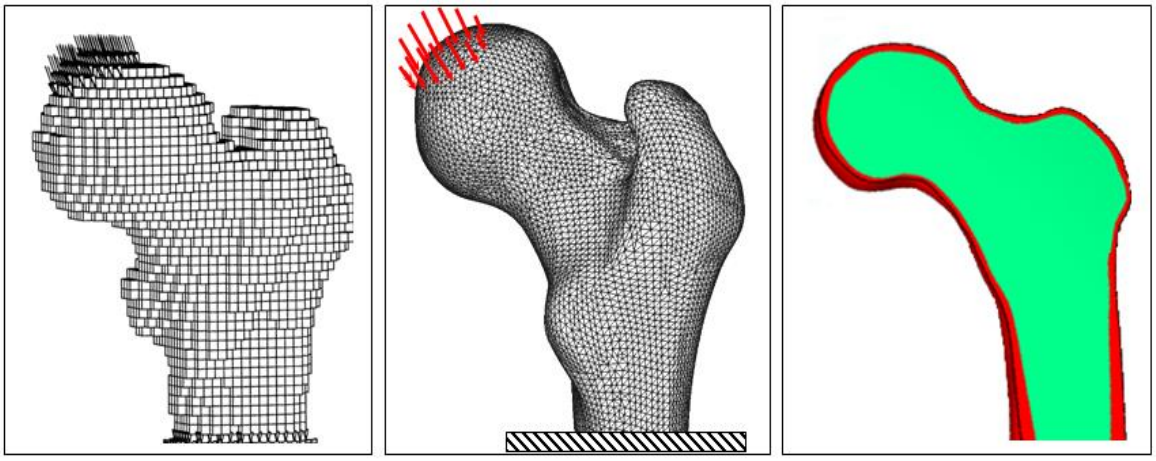

Fig. 3 FE model of the left proximal femur of Subject B (male, age 61) generated from CT scan data obtained in vitro. Displacement was applied to the femoral head, as indicated by the arrows, and the distal portion of the model was restrained (Keyak and Falkinstein 2003): (a) 3D model of Keyak and Falkinstein (2003), (b) Present 3D model and (c) Cross section showing femur partition into cortical and trabecular regions

proposed femur fracture modeling approach will remain unchanged. The aim here was not to simulate the fracture behaviour of Keyak and Falkinstein (2003) femur and perform direct comparative study with experimental results. The focus was to check the validity of the model to

Table 1 Material properties for bone used for the simulation

	Notation	Cortical	Trabecular	Source
General parameters				
Elastic modulus (Initial value)	E (GPa)	15	3	Keyak and Falkinstein (2003)
Poisson ratio	ν	0.3	0.4	Keyak and Falkinstein (2003)
Age	*Age*	61	61	Keyak and Falkinstein (2003)
Damage law parameters				
Critical damage at fracture in tension	D_c^T	0.95	0.95	Pattin *et al.*(1996)
Critical damage at fracture in compression	D_c^C	0.5	0.5	Hambli (2011a, 2011b)
Damage exponent	n	1.25	2	Wolfram *et al.*(2011)
Damage strain threshold	ε_0	0.001	0.001	Wolfram *et al.*(2011)
Strain at fracture in tension	ε_f^T	0.0157	0.025	Wolfram *et al.*(2011) Parsamian (2002)
Strain at fracture in compression	ε_f^C	0.025	0.04	Wolfram *et al.*(2011) Parsamian (2002)

predict (i) a plausible realistic complete force-displacement curve and (ii) the progressive crack propagation leading to final fracture pattern.

The 3D model is partitioned into two regions (Fig. 3(c)): trabecular bone and cortical bone. The same constitutive laws were used for both regions (quasi-brittle behaviour law) but with different material averaged homogenized properties (Table 1).

Nodal displacements at 20° to the shaft axis within the plane containing the shaft and cervical axes were applied incrementally to top surface of the femur head till complete fracture and the model were restrained distally. The movement perpendicular to the applied displacements was permitted. Material properties for bone used for the simulation are given in Table 1. In Keyak and Falkinstein (2003) study, local elastic modulus was calculated for each element using relations linking the material properties for each voxel element to bone density. In this preliminary investigation, a homogeneous elastic modulus was applied to the trabecular and cortical bone.

4. Results

Predicted FE force–displacement curve based on Keyak and Falkinstein's specimen are plotted in Fig. 4(a). Typical experimental force-displacement curve of the tested specimen was reported by Keyak in paper (Keyak 2001) (Fig. 4). Current predicted curve shows a same trend compared to the reported experimental one concerning the curve shape and onset of the yielding and the fracture. The FE-based curve exhibits the sharp drop in force during failure that was nearly always seen during mechanical testing.

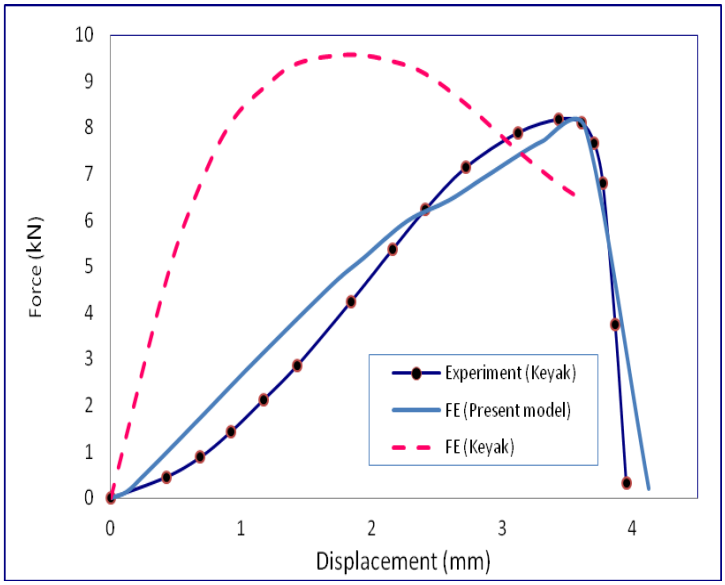

Fig.4 Predicted and experimental force-displacement curves obtained by Keyak (reported in paper Keyak, 2001) and present FE model. Point *B* indicates the occurrence of yielding. Point *C* indicates the occurrence of numerical fracture. From *C* to *D*, the cracks propagates rapidly leading to the drop of the curve (Complete fracture of the femur)

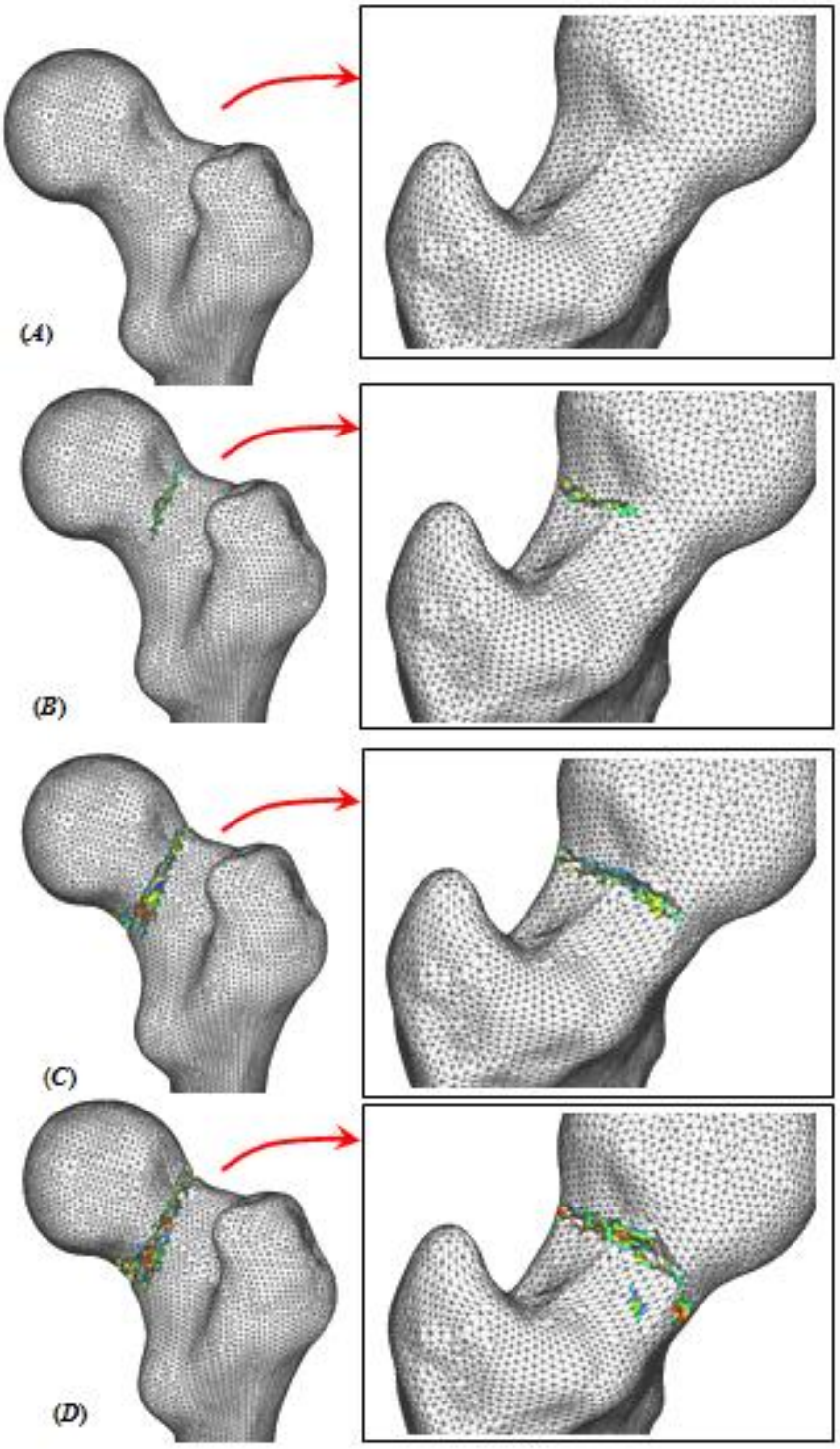

Fig. 5 Cracks propagation sequences in relation with the force-displacement curve. The predicted complete fracture pattern of the femur is given in Fig. 6

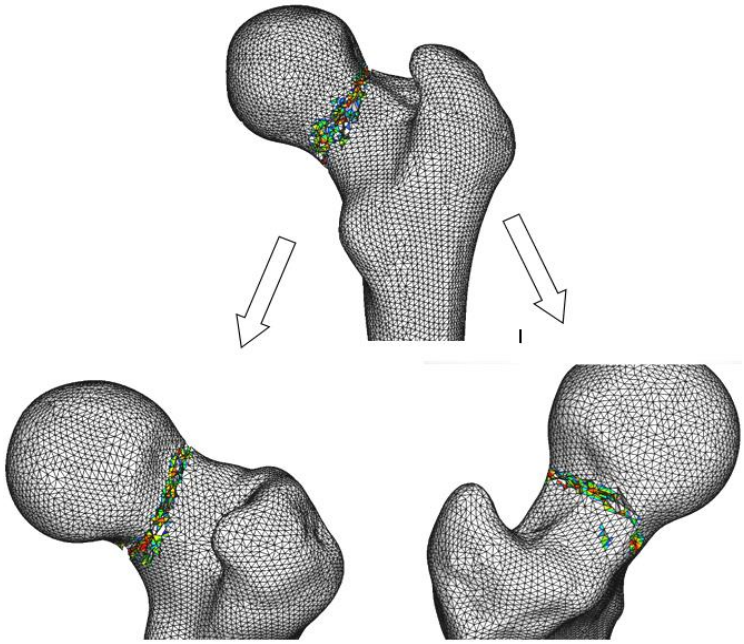

Fig. 6. Predicted fracture patter from different angles

The propagation of the cracks within the femur in relation with the force-displacement curve position is plotted in Fig. 5. In the yielding stage (*B*), the crack is initiated locally at the superior cortex located at the maximum tensile strains. After the yielding phase, the crack continues to grow rapidly, following a perpendicular path to the surfaces leading to complete separation of the proximal femur.

Depending on the boundary conditions, femoral geometry and the bone properties, different fracture pattern can be observed experimentally and the one obtained here (Fig. 6) corresponds to a sub-capital fracture with stage II of Garden classification (Garden 1961) (complete fracture with non-displacement). Such fracture pattern prediction is useful to assist in decision-making on the surgeon's choice of a specific-patient operative treatment.

Predicted results showed that the catastrophic failure occurred in the form of localized crack bands located in the subcapital region. The damage distribution sequences of the specimen (Fig. 5) indicate that a damage accumulation occurred during the loading which ultimately formed a high strain concentration region in the form of shear band (Fig. 6). Bone, as a biological tissue, possesses a very complex hierarchical structure. Its behavior is subjected to excessive mechanical load is characterized by diffuse microcracking that later localizes in relatively narrow zones, referred to as the fracture process zones. This region was the origin of a major crack that resulted in a catastrophic failure.

5. Conclusions

Predicted force-displacement curve shows a same trend as observed experimental ones concerning the curve shape and onset of the yielding Keyak (2001). The FE-based curve exhibits

the sharp drop in force during failure that was nearly always seen during mechanical testing in quasi-static experiment (low strain rates). A more physical approach to determine the value of the fracture force is to consider the maximum force from the force–displacement curve before the drop due to propagation of the cracks. The results of this paper shows that the force-displacement curve and the fracture pattern predicted using the proposed model is more adequate than the results presented in Keyak (2001) and Keyak and Falkinstein (2003).

The predicted fracture pattern corresponds to the path of the cracks after total separation of the fractured finite elements of the mesh. Our results predicted progressive fracture process depending on the femur head displacement value (Fig. 5). The predicted cracks path follow an oblique line with an angle with the horizontal plane greater than 60° (Pauwels type III) from the inner surface of the neck (basal) to the outer surface towards the greater trochanter (Fig. 6).

A limitation of the proposed model lies in the assignment of local heterogeneous and anisotropic material properties in the current FE analysis. A number of relationships were proposed by several authors to convert the CT number of every FE of the mesh to bone material properties such as elastic modulus, strain at fracture, yield stress, anisotropy directions. The focus here was to develop and test the ability of the CDM in simulating the progressive and complete bone fracture and predict plausible force-displacement curve and fracture pattern rather than developing a specific FE model. Nevertheless, the overall structure of the proposed femur fracture modeling approach will remain unchanged. There will be still a need to perform FE simulations to predict the fracture conditions of human proximal femurs under a given boundary risk (stance, side fall). Current published FE models describing proximal femur fracture can be significantly improved to achieve a better description of bone failure, as no standardized FE approach exists for assessing fracture initiation and propagation within bone. Proposed model contributes toward the development of enhanced FE algorithms to perform such prediction with a good compromise between complexity and accuracy of the simulation.

References

Abdel-Wahab, A.A. and Silberschmidt, V.V. (2011), "Numerical modeling of impact fracture of cortical bone tissue using X-FEM", *J. Theor. Appl. Mech.*, **49**(3), 599-619.

Baca, V., Horak, Z., Mikulenka, P. and Dzupa, V. (2008), "Comparison of an inhomogeneous orthotropic and isotropic material models used for FE analyses", *Med. Eng. Phys.*, **30**, 924–930.

Bayraktar, H.H., Morgan, E.F., Niebur G.L., Morris, G.E., Wong, E.K. and Keaveny, T.M. (2004), "Comparison of the elastic and yield properties of human femoral trabecular and cortical bone tissue", *J. Biomech*., **37**, 27–35.

Bessho, M., Ohnishi, I., Matsuyama, J., Matsumoto, T., Imai, K. and Nakamura, K. (2007), "Prediction of strength and strain of the proximal femur by a CT-based finite element method", *J. Biomech*., **40**, 1745–1753.

Burr, D.B. (1993), "Remodeling and the repair of fatigue damage", *Calcified Tissue Int.*, **53**(1), S75-S81**.**

Cody, D.D., Gross, G.J., Hou, F.J., Spencer, H.J., Goldstein, S.A. and Fyhrie, D. (1999), "Femoral strength is better predicted by finite element models than QCT and DXA", *J. Biomech.*, **32**, 1013–1020.

Currey, J.D. (1990), "Physical characteristics affecting the tensile failure properties of compact bone", *J. Biomech*., **23**(8), 837–844.

Currey, J.D. (2002), *Bones: Structure and mechanics*, Princeton University Press, Princeton.

Chaboche, J.L. (1981), "Continuum damage mechanics a tool to describe phenomena before crack initiation", *Nucl. Eng. Des.*, **64**, 233–247.

Crawford, R.P., Cann, C.E. and Keaveny, T.M. (2003), "Finite element models predict in vitro vertebral body compressive strength better than quantitative computed tomography", *Bone*, **33**, 744–750.

Dragomir-Daescu, D., Op Den Buijs, J., McEeligot, S., Dai, Y., Entwistle, R.C., Salas, C., Melton, III J., Bennet, E., Khosla, S. and Amin, S. (2010), "Robust QCT/FEA models of proximal femur stiffness and fracture load during a sideways fall on the hip", *Ann. Biomed. Eng.*, **39**(2), 742-755.

Ford, C.M., Keaveny, T.M. and Hayes, W.C. (1996), "The effect of impact direction on the structural capacity of the proximal femur during falls", *J. Bone Miner. Res.*, **11**, 377–383.

Garden, R. (1961), "Low-angle fixation in fractures of the femoral neck", *J. Bone Joint Surg. Br.*, **43**, 647–661.

Hambli, R., Bettamer, A. and Allaoui, S. (2012), "Finite element prediction of proximal femur fracture pattern based on orthotropic behaviour law coupled to quasi-brittle damage", *Med. Eng. Phys.*, **34**(2), 202-210.

Hambli, R. (2011a), "Multiscale prediction of crack density and crack length accumulation in trabecular bone based on neural networks and finite element simulation", *Int. J. Numer. Method. Biomed. Eng.*, **27**(4), 461–475.

Hambli, R. (2011b), "Apparent damage accumulation in cancellous bone using neural networks", *J. Mech. Behav. Biomed. Mater.*, **4**(6),868-878.

Juszczyk, M.M., Cristofolini, L. and Viceconti, M. (2011), "The human proximal femur behaves linearly elastic up to failure under physiological loading conditions", *J. Biomech.*, **44**(12), 2259-2266.

Kaneko, T.S., Pejcic, M.R., Tehranzadeh, J. and Keyak, J.H. (2003), "Relationships between material properties and CT scan data of cortical bone with and without metastatic lesions", *Med. Eng. Phys.*, **25**(6), 445-454.

Kotha, S.P. and Guzelsu, N. (2003), "Tensile damage and its effects on cortical bone", *J. Biomech.*, **36**(11), 1683–1689.

Keaveny, T.M., Wachtel, E.F., Ford, C.M. and Hayes, W.C. (1994), "Differences between the tensile and compressive strengths of bovine tibial trabecular bone depend on modulus", *J. Biomech.*, **27**, 1137–1146.

Keaveny, T.M., Wachtel, E.F. and Kopperdahl, D.L. (1999), "Mechanical behavior of human trabecular bone after overloading", *J. Orthopaed. Res.*, **17**, 346–353.

Keaveny, T.M., Morgan, E.F., Niebur, G.L. and Yeh, O.C. (2001), "Biomechanics of trabecular bone", *Ann. Biomed. Eng.*, **3**, 307–333.

Keyak, J.H. (2001), "Improved prediction of proximal femoral fracture load using nonlinear finite element models", *Med. Eng. Phys.*, **23**, 165–173.

Keyak, J.H. and Falkinstein, Y. (2003), "Comparison of in situ and in vitro CT scan-based finite element model predictions of proximal femoral fracture load", *Med. Eng. Phys.*, **25**, 781–787.

Link, M., Vieth, V., Langenberg, R., Meier, N., Lotter, A., Newitt, D. and Majumdar, S. (2003), "Structure analysis of high resolution magnetic resonance imaging of the proximal femur: in vitro correlation with biomechanical strength and BMD", *Calcified Tissue Int.*, 72,156–165.

Lemaitre, J. (1985), "A continuous damage mechanics model for ductile fracture", *J. Eng. Mater. Technol.*, **107**, 83-89.

Lotz, J.C, Cheal, E.J. and Hayes, W.C. (1991a), "Fracture prediction for the proximal femur using finite element models: Part I - Linear analysis", *J. Biomech. Eng.*, **113**, 353–360.

Lotz, J.C., Cheal, E.J. and Hayes, W.C. (1991b), "Fracture prediction for the proximal femur using finite element models: Part II - Nonlinear analysis", *J. Biomech. Eng.*, **113**, 361–365.

Lotz, J.C., Cheal, E.J. and Hayes, W.C. (1995), "Stress distributions within the proximal femur during gait and falls: implications for osteoporotic fracture", *Osteopor Int.*, **5**, 252–261.

Malik, L., Stover, M., Martin, B. and Gibeling, C. (2003), "Equine cortical bone exhibits rising R-curve fracture mechanics", *J. Biomech.*, **36**, 191–198.

Mazars, J. and Pijaudier-Cabot, G. (1996), "From damage to fracture mechanics and conversely: A combined approach", *Int. J. Solid Struct.*, **33**, 3327-3342.

Nagaraja, S., Couse, T.L. and Guldberg, R.E. (2005), "Trabecular bone microdamage and microstructural stresses under uniaxial compression", *J. Biomech.*, **38**, 707–716.

Nalla, K., Kruzic, J., Kinney, H. and Ritchie, O. (2005), "Mechanistic aspects of fracture and R-curve behavior in human cortical bone", *Biomater*., **26**, 217–231.

Ota, T., Yamamoto, I. and Morita, R. (1999), "Fracture simulation of femoral bone using finite-element method: How a fracture initiates and proceeds", *J. Bone Miner. Metab*., **17**(2), 108–112.

Pattin, C.A., Caler, W.E. and Carter, D.R. (1996), "Cyclic mechanical property degradation during fatigue loading of cortical bone", *J. Biomech.*, **29**, 69–79.

Parsamian, G.P. (2002), *Damage mechanics of human cortical bone: Phd*, College of Engineering and Mineral Resources at West Virginia University.

Peng, L., Bai, J., Zeng, X. and Zhou, Y. (2006), "Comparison of isotropic and orthotropic material property assignments on femoral finite element models under two loading conditions", *Med. Eng. Phys.*, **28**, 227–233.

Reilly, D.T. and Burstein, A.H. (1974), "Review article. The mechanical properties of cortical bone", *J. Bone Jt. Surg. Am.*, **56**, 1001–1022.

Reilly, D.T. and Burstein, A.H. (1975), "The elastic and ultimate properties of compact bone tissue", *J. Biomech.*, **8**, 393–405.

San Antonio, T., Ciaccia, M., Müller-Karger, C. and Casanova, E. (2012), "Orientation of orthotropic material properties in a femur FE model: A method based on the principal stresses directions", *Med. Eng. Phys.*, **34**(7), 914-919.

Schileo, E., Taddei, F., Cristofolini, L. and Viceconti, M. (2008), "Subject-specific finite element models implementing a maximum principal strain criterion are able to estimate failure risk and fracture location on human femurs tested in vitro", *J. Biomech*., **41**(2), 356-367.

Taylor, D. and Lee, T.C. (2003), "A crack growth model for the simulation of fatigue in bone", *Int. J. Fatigue*, **2**, 387–395.

Taddei, F., Cristofolini, L., Martelli, S., Gill, H. and Viceconti, M. (2006), "Subject-specific finite element models of long bones: an in vitro evaluation of the overall accuracy", *J. Biomech*., **39**, 2457–2467.

Tellache, M., Pithioux, M., Chabrand, P. and Hochard, C. (2009), "Femoral neck fracture prediction by anisotropic yield criteria", *Eur. J. Comput. Mech*., **1**, 33-41.

Ural, A. and Vashishth, D. (2007), "Anisotropy of age-related toughness loss in human cortical bone: A finite element study", *J. Biomech*., **40,** 1606–1614.

Vashishth, D., Tanner, E. and Bonfield, W. (2003), "Experimental validation of a microcracking-based toughening mechanism for cortical bone", *J. Biomech*., **36**(1), 121–124.

Vashishth, D., Behiri, J.C. and Bonfield, W. (1997), "Crack growth resistance in cortical bone: Concept of microcrack toughening", *J. Biomech.*, **30**(8), 763–769.

Verhulp, E., van Rietbergen, B. and Huiskes, R. (2006), "Comparison of micro-level and continuum level voxel models of the proximal femur", *J. Biomech.* **39**, 2951–2957.

Wang, X., Zauel, R. and Fyhrie, D.P. (2008a), "Postfailure modulus strongly affects microcracking and mechanical property change in human iliac cancellous bone: A study using a 2D nonlinear finite element method", *J. Biomech*., **41**, 2654– 2658.

Wang, X., Zauel, R., Sudhaker Rao, D. and Fyhrie, D.P. (2008b), "Cancellous bone lamellae strongly affect microcrack propagation and apparent mechanical properties: Separation of patients with osteoporotic fracture from normal controls using a 2D nonlinear finite element method (biomechanical)", *Bone*, **42**(6), 1184–1192.

Wolfram, U., Wilke, H.J. and Zysset, P.K. (2011), "Damage accumulation in vertebral trabecular bone depends on loading mode and direction", *J. Biomech.*, **44**(6),1164-1169.

Yang, D., Cox, N., Nalla, K. and Ritchie, O. (2006), "Re-evaluating the toughness of human cortical bone", *Bone*, **38**, 878–887.

Yang, H., Shen, L., Demetropoulos, K., King, I., Kolodziej, P., Levine, S. and Fitzgerald, J. (1996), "The relationship between loading conditions and fracture patterns of the proximal femur", *J. Biomech. Eng*., **118**, 575–578.

Yosibash, Z., Tal, D. and Trabelsi, N. (2010), "Inhomogeneous orthotropic material properties high-order finite-element analysis with inhomogeneous orthotropic material properties", *Phil. Trans. R. Soc. A*, **368**, 2707-2723.

Zioupos, P., Tong Wang, X. and Currey, J.D. (1996), "Experimental and theoretical quantification of the development of damage in fatigue tests of bone and antler", *J. Biomech*., **29**(8), 989-1002.

YY